

Efficiency of Feynman’s quantum computer

R. J. Costales,^{1,*} A. Gunning,^{1,†} and T. Dorlas¹

¹*School of Theoretical Physics, Dublin Institute for Advanced Studies, 10 Burlington Road, Dublin D04 C932, Ireland.*

(Dated: January 23, 2025)

Feynman’s circuit-to-Hamiltonian construction enables the mapping of a quantum circuit to a time-independent Hamiltonian. This model introduces a Hilbert space made from an ancillary clock register tracking the progress of the computation. In this paper, we explore the efficiency, or run-time, of a quantum computer that directly implements the clock system. This relates to the model’s probability of computation completion which we investigate at an established optimal time for an arbitrary number of gates k . The relationship between the run-time of the model and the number of gates is obtained both numerically and analytically to be $O(k^{5/3})$. In principle, this is significantly more efficient than the well investigated Feynman-Kitaev model of adiabatic quantum computation with a run-time of $O(k^4)$. We address the challenge which stems from the small window that exists to capture the optimal stopping time, after which there are rapid oscillations of decreasing probability amplitude. We establish a relationship for the time difference between the first and second maximum which scales as $O(k^{1/3})$.

I. INTRODUCTION

In 1981, Feynman highlighted the physical limitations of classical computers and proposed using quantum computers to simulate quantum systems [1]. In searching for a system Hamiltonian that could perform as a computer, he proposed the original clock Hamiltonian for the purposes of circuit model quantum computation. Since then, there has been significant interest in exploiting his scheme. Aharonov et al. used the model to show the equivalence of adiabatic quantum computation and the circuit model [2]. Kitaev et al. demonstrated the local Hamiltonian problem is QMA-complete for open quantum systems [3]. The clock model has been more recently studied in several quantum complexity results [4–7], improving gap bounds [6], establishing a relationship with quantum walk Hamiltonians [6, 8] and extensions to open quantum systems [9]. Modifications have also been made to the model to incorporate forward biasing, additional qubits [6, 10], combinations of several clock registers [5] to improve success probability, a railroad switch gadget for physical implementations [10–13] and noise-assisted transport to remove trapping regions in the clock register [14]. Feynman’s original work has also inspired alternative constructions such as the ‘space-time circuit-to-Hamiltonian’ model in which the global clock is replaced by local clocks for each information carrying particle [7, 15–17], as well as models incorporating tensor networks and use of quantum fault tolerance [18]. The greatest interest in the Feynman-Kitaev model has followed from Aharonov’s work regarding adiabatic computation with most research being devoted to improving the minimum spectral gap bounds on this model [2, 6, 8, 17, 19–24]. The heavy analysis on this aspect of the adiabatic model has been in an effort to understand its efficiency (run-time) which was

found to be of the order $O(k^4)$ [2, 23, 24] where k is the number of unitary operations.

In this paper, we provide a direct comparison with the adiabatic model by considering the straightforward circuit implementation of Feynman’s original clock Hamiltonian. The major contribution of this work is in demonstrating that the efficiency of the clock model is a significant improvement over the adiabatic implementation.

A. Feynman’s Clock Space

Feynman’s clock model exploits the circuit model of quantum computation, originally introduced by Feynman and Deutsch [25, 26]. Here, a calculation is performed by preparing a set of n logical qubits in the computational basis state $|\psi_{\text{in}}\rangle = |0_1 0_2 \dots 0_n\rangle$ and acting on this state with a suitably chosen unitary operator \hat{U} to obtain a final state $|\psi_{\text{out}}\rangle = \hat{U} |\psi_{\text{in}}\rangle$. The unitary operator is constructed in such a way that a measurement of this final state in the computational basis yields the desired result of the computation. Similar to the operation of NOT, AND and OR gates being sufficient to generate any logical operation, it has been proven that one can approximate any given such unitary matrix \hat{U} by a sequence of unitary gates $\hat{U}_1, \hat{U}_2, \dots, \hat{U}_{k-1}, \hat{U}_k$, chosen from a limited set of basic unitary matrices known as a universal set of quantum gates acting individually on a small subset of the logical qubits [27, 28]. Replacing \hat{U} by this sequence of quantum gates, the resulting output state is $|\psi_{\text{out}}\rangle = \hat{U}_k \hat{U}_{k-1} \dots \hat{U}_2 \hat{U}_1 |\psi_{\text{in}}\rangle$. The successive operation of quantum gates can be represented in a quantum circuit diagram as in Fig. I A. Feynman showed that it is also possible to achieve quantum computation by mapping the quantum circuit to a continuous-time evolution with a time-independent Hamiltonian. Here, an initial state evolves according to Schrodinger’s equation while still implementing a discrete sequence of unitaries [1]. There is advantage in this construction as it allows simulation of time-dependent quantum mechanics using a time-independent framework, having no requirement for active driving fields to perform logical operations [2, 29, 30].

Feynman’s circuit-to-Hamiltonian construction involves

* These authors have contributed equally to this work; Presently at the London Centre for Nanotechnology and the Department of Physics and Astronomy, University College London.

† These authors have contributed equally to this work; Presently at the Department of Physics, University of Oxford.

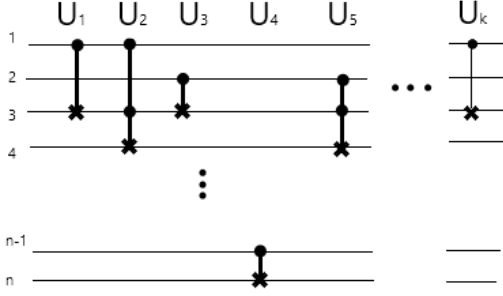


FIG. 1. Schematic of a quantum circuit depicting the succession of \hat{U}_k operators we want to perform on the input state, $|\psi_{in}\rangle$, of n qubits in our register to arrive at our desired output state, $|\psi_{out}\rangle$.

the composition of unitary operators in the following way. Let $\hat{U}_1, \hat{U}_2, \dots, \hat{U}_{k-1}, \hat{U}_k$ be the succession of operations we want to operate on the input state of the n -qubits in our ‘register’ $|\psi_{in}\rangle$. Adjacent to the register, we add an entirely new set of $k + 1$ qubits, called ‘program counter sites’ which live in an ancillary ‘clock space’, separate from the Hilbert space of the register. The purpose of the clock space is to track the progress of the computation. The program counter can be thought of as a particle hopping between sites of a one-dimensional lattice. The states in the clock space are of the form below,

$$\begin{aligned} |0\rangle_c &= |1000\dots00\rangle \\ |1\rangle_c &= |0100\dots00\rangle \\ &\vdots \\ |k-1\rangle_c &= |00\dots0010\rangle \\ |k\rangle_c &= |00\dots0001\rangle. \end{aligned}$$

Feynman proposed that we initialise our clock space in the state $|0\rangle_c$ at the beginning of our computation. At each step of the computation i.e. as each operator U_j acts on the register of n qubits, the counter moves to the subsequent $|j\rangle_c$ state of our clock space. Eventually, the program counter evolves to the final state of the clock space $|k\rangle_c$ with the final operator U_k acting on the register, at which stage the computation is complete. The register must be observed immediately to ensure that the program counter does not return back down the program line. The complete Hamiltonian, describing the evolution of the register qubits and the clock qubits, is given by,

$$\hat{H} = \sum_{i=0}^{k-1} \hat{q}_{i+1}^\dagger \hat{q}_i \hat{U}_{i+1} + \text{H.C} \quad (1)$$

$$= \sum_{i=0}^{k-1} \left(|i+1\rangle \langle i|_c \otimes \hat{U}_{i+1} + |i\rangle \langle i+1|_c \otimes \hat{U}_{i+1}^\dagger \right). \quad (2)$$

Here \hat{q}_i^\dagger and \hat{q}_i are creation and annihilation operators at the i -th clock site, so that $\hat{q}_{i+1}^\dagger \hat{q}_i$ moves the counter one site to the

right. Note that the Hermitian conjugate term $\hat{q}_i^\dagger \hat{q}_{i+1}$ occurring in the H.C. term moves the counter one site to the left, so that the clock can also move back in time.

In summary, our Hilbert space for this model $\mathcal{H} = \mathcal{H}_{\text{clock}} \otimes \mathcal{H}_{\text{register}}$ can be broken into two spaces, a clock register whose $k + 1$ orthonormal states track the linear progress of the computation and a data register that contains the n computational qubits that our unitary gates act on. During the computation, we will evolve some initial state $|\psi_0\rangle = |0\rangle_c \otimes |\psi_{in}\rangle$ with our clock Hamiltonian and we will arrive at some resulting state of the form,

$$|\psi_t\rangle = |t\rangle_c \otimes (\hat{U}_t, \dots, \hat{U}_1 |\psi_{in}\rangle), t = 0, 1, \dots, k, \quad (3)$$

where $|\psi_k\rangle = |k\rangle_c \otimes |\psi_{out}\rangle$ is our final state that contains the answer to our computation [6].

In this paper, we aim to examine the efficiency of Feynman’s quantum computer. For our purposes, this is defined to be the run-time or the time of computation completion for our model. We will work this out by examining the probability $P_k(t)$ that the initial state $|\psi_0\rangle$ of our computation evolves to the final state $|\psi_k\rangle$ at time t .

B. Adiabatic Quantum Computation

The significance of our results for the run-time of Feynman’s clock model in Section II becomes evident when we compare with a model that has been more heavily investigated - adiabatic quantum computing. We include this particular model as its efficiency has been investigated in great detail with regards to evolution using a clock space [2, 17, 20, 21]. Aharonov et al. [2] showed the computational equivalence between adiabatic computation and the quantum circuit model, by demonstrating an adiabatic evolution with the same output as that of an arbitrary quantum circuit. The critical element was Feynman’s circuit-to-Hamiltonian construction and their method is laid out in Appendix A. It was shown by Aharonov [2] and Kitaev [3] that the run-time for this model is polynomial in the number of operations k by analysing $H_{\text{clock}}(s)$,

$$\hat{H}_{\text{clock}}(s) = \begin{bmatrix} s/2 & -s/2 & & & & & \\ -s/2 & 1 & -s/2 & & & & \\ & -s/2 & 1 & -s/2 & & & \\ & & \ddots & \ddots & \ddots & & \\ & & & -s/2 & 1 & -s/2 & \\ & & & & -s/2 & 1 - s/2 & \end{bmatrix}, \quad (4)$$

where s is a rescaled time parameter.

The latter authors estimated that the minimum gap Δ of \hat{H}_{clock} to be bounded below by $1/(144k^2)$. This bound was improved by Dooley et al. [20] to $\pi^2/(8k^2) \sim 1.23k^{-2}$. By the adiabatic theorem (see Born [24]) the time needed for adiabatic evolution is proportional to Δ^{-2} . This relationship requires that the spectrum is discrete, and that the eigenvalues do not overlap other than at a few points in time, which is true in this case [20]. (Note that the theorem by Born

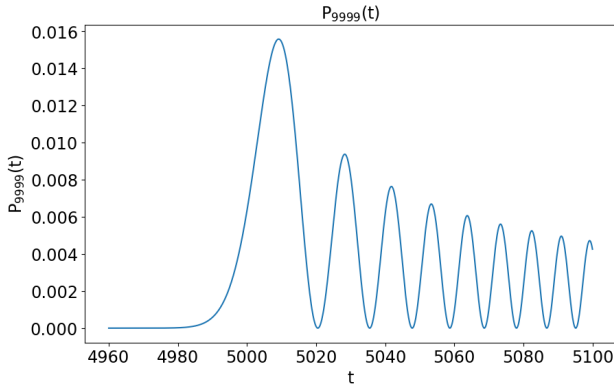


FIG. 2. Plot of $P_k(t)$ for $k=9999$ operators generated from (10). The first local maximum of $P_k(t)$ is also the global maximum and can be represented by $P_k(\tau)$. The amplitude of each local maxima decreases with time if the program is not immediately stopped at $t = \tau$.

Hamiltonian $\hat{H}_{\text{clock}}(s)$ in (4) to determine the run-time for the model.

This matrix obeys the following eigenvalue equation,

$$\begin{aligned} \hat{H}_{\text{clock}} |\varphi_j\rangle &= \lambda_j |\varphi_j\rangle, \\ e^{-i\hat{H}_{\text{clock}}t} |\varphi_j\rangle &= e^{-i\lambda_j t} |\varphi_j\rangle, \end{aligned}$$

for $j = 0, \dots, k$.

Using a Fourier transformation, the eigenvalues and eigenstates of the effective Hamiltonian are found to be,

$$\lambda_j = 2 \cos \frac{\pi(j+1)}{k+1}; \quad |\varphi_j\rangle = \frac{2}{k+1} \begin{bmatrix} \sin \frac{\pi(j+1)}{k+1} \\ \sin \frac{2\pi(j+1)}{k+1} \\ \vdots \\ \sin \frac{k\pi(j+1)}{k+1} \end{bmatrix}. \quad (9)$$

The probability $P_k(t)$ can now be calculated using (8),

$$P_k(t) = \left| \frac{2}{k+1} \sum_{j=0}^k e^{-i\lambda_j t} \sin^2 \frac{\pi(j+1)}{k+1} (-1)^j \right|^2. \quad (10)$$

Using (10) for a large number of operations, $k \gg 1$, the optimal stopping time τ is found to be at the first local maximum of $P_k(t)$ as shown in Fig.2. There is a small window to capture the first maximal peak after which there are rapid oscillations of probability which decrease in amplitude with time. Numerically, the optimal stopping time is found to grow linearly with the number of operations, $\tau \propto 0.50k$, as shown in Fig.3.

The probability $P_k(\tau)$ can be plotted against k to derive the relationship between probability of computation completion at the optimal time and the number of operations. Numerically, we find that there is an inverse cubic relationship between them, $P_k(\tau) = \alpha k^{-2/3}$, as shown in Fig.4. To obtain a success probability of order 1 for our $P_k(\tau)$, one must repeat

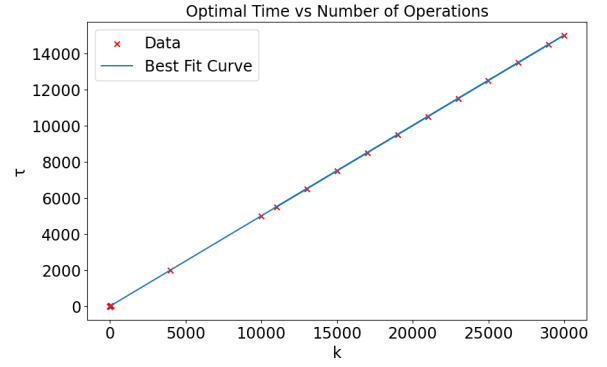


FIG. 3. Scatter plot of the optimal time τ which is found by maximising $P_k(t)$ for a given number of operations k . A linear relationship is observed between τ and k with best fit parameters $\tau = 0.50k + 2.37$.

the calculation $O(k^{2/3})$ times, leading to an estimated run-time of $O(k^{5/3})$. This is a significant improvement over adiabatic evolution, which has a running time of $O(k^4)$, as analysed by Aharonov et. al. [2] (see also [20]). Analytically verifying the relationship with $P_k(\tau)$ and k , we use Taylor expansions of trigonometric functions to express (10) in the form,

$$P_k(\tau) = \left| \frac{4}{k+1} \sum_{p=0}^{\frac{k}{2}} \cos^2 \left(\frac{\pi(2p-1)}{2(k+1)} \right) \times \cos \left(\frac{\pi^3}{6(k+1)^2} \left(p - \frac{1}{2} \right)^3 \right) \right|^2. \quad (11)$$

This summation form can be approximated by asymptotic analysis, writing it in the form of a Riemann integral assuming that we have a large number of operations, $k \gg 1$: see Appendix D. The result is,

$$P_k(\tau) \approx 5.14k^{-2/3}. \quad (12)$$

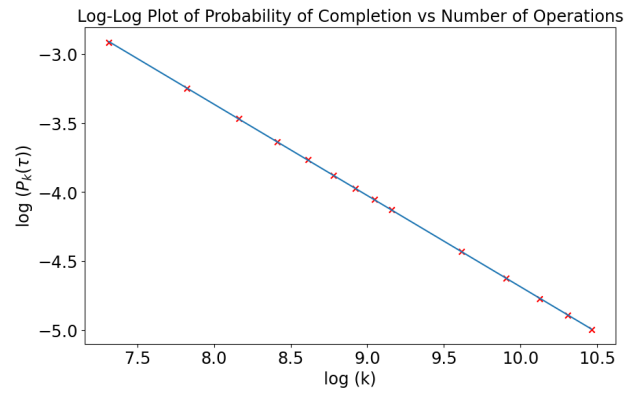


FIG. 4. Log-Log scatter plot of the optimal probability $P_k(\tau)$ which is found by maximising $P_k(t)$ for a given number of operations k . An inverse cubic relationship is observed between $P_k(\tau)$ and k with best fit parameters $P_k(\tau) = 6.76k^{-2/3}$.

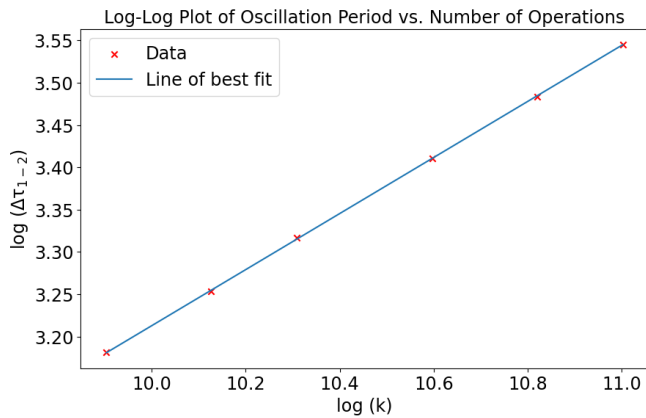


FIG. 5. Log-Log plot of time difference, $\Delta\tau_{1-2}$, between the optimal stopping time, τ_1 , and the next optimal time τ_2 against number of operations, k .

C. Period of Oscillations

An initial concern relates to the small window to capture the first maximal peak in Fig. 2 which is followed by large oscillations in decreasing amplitude. It is important to investigate the period of the oscillations after the first maximum of $P_k(t)$, as this indicates how accurately one must be able to determine the stopping time τ of the computer (to measure the output state). If the register is not stopped at the optimal time, τ_1 , but is instead stopped at the next optimal time, τ_2 , then the probability $P_k(\tau_2)$ is lower, i.e. it is less likely that the operations have been completed. If $\tau_1 \approx \frac{1}{2}(k+2)$ is the time where the first maximum is attained, we write $\tau_2 \approx \frac{1}{2}(k+2)(1+\delta)$, and $\Delta\tau_{1-2} \approx \delta \times \frac{k+2}{2}$. Numerically plotting the time difference between the first and second maximum as seen in Fig.5 we find that,

$$\Delta\tau_{1-2} = \beta k^{1/3}. \quad (13)$$

In Appendix E we obtain the analytical prediction $\Delta\tau_{1-2} = 1.115(k+2)^{1/3}$. This means that one needs to be able to stop the computer at a time accurate up to a fraction of $k^{1/3}$. This is much shorter than the stopping time but is still a promising scaling as it increases with k . As the number of required operations k grows, the time difference between the first two local maxima also grows, ensuring the optimal time is easier to capture. This also allows the opportunity to capture the register at the second local maximum, removing the need to restart the computation if the optimal stopping time is missed. Assuming that the accuracy with which the time of measurement is determined is independent of k , the scaling found here is optimistic for future implementations.

III. DISCUSSION

We have presented the theory behind Feynman's theoretical construction for a quantum computer, wherein a quantum circuit is mapped to a time-independent Hamiltonian by use of a clock space. A formula is established for the probability, $P_k(t)$, that the desired computation is complete at time t for a quantum computer which executes k number of operations. The analysis here is reminiscent of that for state transfer in quantum spin systems [31–33]. We demonstrate that the computation is complete with probability $O(k^{-2/3})$ in optimal time $\tau = O(k)$. For a success probability of order 1, the calculation must be repeated $O(k^{2/3})$ times, leading to an estimated run time of $O(k^{5/3})$. This is a significant improvement over adiabatic evolution with a run time $O(k^4)$. We deal with an ideal machine and the superiority of the model is dependent on whether this can be implemented in practice. Although Feynman's clock model has been appreciated on a theoretical level for decades, it is only recently receiving necessary experimental attention. The major challenge with implementation stems from the controlled interaction between the clock register and the unitary gates. Previous avenues of implementation for Hamiltonian quantum computing have included multi-particle quantum walks with interactions using ultra cold bosonic atoms [34, 35]. Most interesting to us is a two dimensional lattice construction using a time-independent Hamiltonian by Lloyd and Terhal [13]. It has been recently expanded on by Ciani et al. in [12] with a proposal for a superconducting transmon qubit implementation, that exploits the railroad switch modification of the clock register introduced by Nagaj [10, 11] for universal quantum computation. The implementation used is similar to those in [7, 8, 15]. Ciani provides a direct comparison to the multi-clock Lloyd–Terhal construction by investigating a physical implementation of the single clock Feynman model which we explore here. They discuss how to achieve the weaker hopping interactions and strong-attractive cross Kerr coupling necessary between transmons in this scheme. An initial investigation into the error rates related to gate implementation is discussed in [12], but a more thorough analysis into fault tolerance and leakage protection for this 2D rail-road implementation can be found in [13]. Incorporating quantum error correction explicitly into Feynman's model remains an open question that requires further investigation. It is clear these new routes of implementation for Feynman's computer reinforces the importance of further investigation into this efficient model.

ACKNOWLEDGEMENTS

The authors would like to thank Steve Campbell for valuable discussions and feedback.

[1] Richard P. Feynman, "Quantum Mechanical Computers," *Optics News* **11**, 11–20 (1985).

[2] D. Aharonov, W. van Dam, J. Kempe, Z. Landau, S. Lloyd, and O. Regev, "Adiabatic quantum computation is equivalent

- to standard quantum computation,” in *45th Annual IEEE Symposium on Foundations of Computer Science* (2004) pp. 42–51.
- [3] Alexei Yu Kitaev, Alexander Shen, and Mikhail N Vyalii, *Classical and quantum computation*, 47 (American Mathematical Soc., 2002).
- [4] Sean Hallgren, Daniel Nagaj, and Sandeep Narayanaswami, “The local hamiltonian problem on a line with eight states is qma-complete,” arXiv preprint arXiv:1312.1469 (2013).
- [5] David Gosset and Daniel Nagaj, “Quantum 3-sat is qma₁-complete,” *SIAM Journal on Computing* **45**, 1080–1128 (2016).
- [6] Libor Caha, Zeph Landau, and Daniel Nagaj, “Clocks in feynman’s computer and kitaev’s local hamiltonian: Bias, gaps, idling, and pulse tuning,” *Physical Review A* **97** (2018), 10.1103/physreva.97.062306.
- [7] Nikolas P Breuckmann and Barbara M Terhal, “Space-time circuit-to-hamiltonian construction and its applications,” *Journal of Physics A: Mathematical and Theoretical* **47**, 195304 (2014).
- [8] David Gosset, Barbara M Terhal, and Anna Vershynina, “Universal adiabatic quantum computation via the space-time circuit-to-hamiltonian construction,” *Physical review letters* **114**, 140501 (2015).
- [9] David G Tempel and Alán Aspuru-Guzik, “The kitaev–feynman clock for open quantum systems,” *New Journal of Physics* **16**, 113066 (2014).
- [10] Daniel Nagaj, “Universal two-body-hamiltonian quantum computing,” *Phys. Rev. A* **85**, 032330 (2012).
- [11] Daniel Nagaj, “Fast universal quantum computation with railroad-switch local hamiltonians,” *Journal of Mathematical Physics* **51** (2010), 10.1063/1.3384661.
- [12] Alessandro Ciani, Barbara Maria Terhal, and David Peter DiVincenzo, “Hamiltonian quantum computing with superconducting qubits,” *Quantum science and technology* **4**, 035002 (2019).
- [13] Seth Lloyd and Barbara M Terhal, “Adiabatic and hamiltonian computing on a 2d lattice with simple two-qubit interactions,” *New Journal of Physics* **18**, 023042 (2016).
- [14] Diego De Falco and Dario Tamascelli, “Noise-assisted quantum transport and computation,” *Journal of Physics A: Mathematical and Theoretical* **46**, 225301 (2013).
- [15] Dominik Janzing, “Spin-1/2 particles moving on a two-dimensional lattice with nearest-neighbor interactions can realize an autonomous quantum computer,” *Physical Review A—Atomic, Molecular, and Optical Physics* **75**, 012307 (2007).
- [16] Ari Mizel, MW Mitchell, and Marvin L Cohen, “Energy barrier to decoherence,” *Physical Review A* **63**, 040302 (2001).
- [17] Ari Mizel, Daniel A Lidar, and Morgan Mitchell, “Simple proof of equivalence between adiabatic quantum computation and the circuit model,” *Physical review letters* **99**, 070502 (2007).
- [18] Anurag Anshu, Nikolas P Breuckmann, and Quynh T Nguyen, “Circuit-to-hamiltonian from tensor networks and fault tolerance,” in *Proceedings of the 56th Annual ACM Symposium on Theory of Computing* (2024) pp. 585–595.
- [19] Johannes Bausch and Elizabeth Crosson, “Analysis and limitations of modified circuit-to-hamiltonian constructions,” *Quantum* **2**, 94 (2018).
- [20] Shane Dooley, Graham Kells, Hosho Katsura, and Tony C. Dorlas, “Simulating quantum circuits by adiabatic computation: Improved spectral gap bounds,” *Physical Review A* **101** (2020), 10.1103/physreva.101.042302.
- [21] Percy Deift, Mary Beth Ruskai, and Wolfgang Spitzer, “Improved gap estimates for simulating quantum circuits by adiabatic evolution,” arXiv preprint quant-ph/0605156 (2006).
- [22] Tosio Kato, “On the adiabatic theorem of quantum mechanics,” *Journal of the Physical Society of Japan* **5**, 435–439 (1950).
- [23] Sabine Jansen, Mary-Beth Ruskai, and Ruedi Seiler, “Bounds for the adiabatic approximation with applications to quantum computation,” *Journal of Mathematical Physics* **48** (2007).
- [24] Max Born and Vladimir Fock, “Beweis des adiabatsatzes,” *Zeitschrift für Physik* **51**, 165–180 (1928).
- [25] Richard P Feynman *et al.*, “Simulating physics with computers,” *Int. j. Theor. phys* **21** (2018).
- [26] David Deutsch, “Quantum theory, the church–turing principle and the universal quantum computer,” *Proceedings of the Royal Society of London. A. Mathematical and Physical Sciences* **400**, 117 – 97 (1985).
- [27] David Eliesser Deutsch, “Quantum computational networks,” *Proceedings of the royal society of London. A. mathematical and physical sciences* **425**, 73–90 (1989).
- [28] Michael A Nielsen and Isaac L Chuang, *Quantum computation and quantum information* (Cambridge university press, 2010).
- [29] Jarrod R McClean, John A Parkhill, and Alán Aspuru-Guzik, “Feynman’s clock, a new variational principle, and parallel-in-time quantum dynamics,” *Proceedings of the National Academy of Sciences* **110**, E3901–E3909 (2013).
- [30] Ari Mizel, “Mimicking time evolution within a quantum ground state: Ground-state quantum computation, cloning, and teleportation,” *Phys. Rev. A* **70**, 012304 (2004).
- [31] Matthias Christandl, Nilanjana Datta, Artur Ekert, and Andrew J. Landahl, “Perfect state transfer in quantum spin networks,” *Phys. Rev. Lett.* **92**, 187902 (2004).
- [32] Matthias Christandl, Nilanjana Datta, Tony C Dorlas, Artur Ekert, Alastair Kay, and Andrew J Landahl, “Perfect transfer of arbitrary states in quantum spin networks,” *Physical Review A* **71**, 032312 (2005).
- [33] Sougato Bose, “Quantum communication through an unmodulated spin chain,” *Phys. Rev. Lett.* **91**, 207901 (2003).
- [34] Andrew M Childs, David Gosset, and Zak Webb, “Universal computation by multiparticle quantum walk,” *Science* **339**, 791–794 (2013).
- [35] Yoav Lahini, Gregory R Steinbrecher, Adam D Bookatz, and Dirk Englund, “Quantum logic using correlated one-dimensional quantum walks,” *npj Quantum Information* **4**, 2 (2018).

IV. APPENDIX

Appendix A: Circuit-to-Hamiltonian construction for Adiabatic Evolution

In the adiabatic method one evolves the time-dependent Hamiltonian of the form,

$$H(s) = (1 - s)H_{\text{init}} + sH_{\text{final}},$$

where $s = t/T$ is a rescaled time as in the adiabatic theorem and T is a large final time. During the computation s varies from 0 to 1. One must ensure that the groundstate of H_{init} encodes the initial state of our computation $|\psi_{\text{in}}\rangle = |0_1 0_2 \dots 0_n\rangle$ and that the groundstate of H_{final} has a non-negligible

inner product with the answer of our computation $|\psi_{out}\rangle = \hat{U}_k \dots \hat{U}_2 \hat{U}_1 |\psi_{in}\rangle$. The main ingredient of Aharonov's solution [2] was the incorporation of Feynman's clock space in the following way.

The initial Hamiltonian is given by,

$$H_{\text{init}} = \sum_{i=1}^N |1_i\rangle\langle 1_i| \otimes |0\rangle_c \langle 0|_c + I \otimes \sum_{l=1}^k |l\rangle_c \langle l|_c.$$

(Here $|1_i\rangle\langle 1_i|$ is the projection on the state $|1\rangle$ of the i -th qubit, and acts as the identity on the other qubits.) This Hamiltonian has the required groundstate $|\psi_0\rangle = |0\rangle_c \otimes |\psi_{in}\rangle$. The final Hamiltonian is,

$$H_{\text{final}} = H_{\text{Feynman}} + \sum_{i=1}^N |1_i\rangle\langle 1_i| \otimes |0\rangle_c \langle 0|_c.$$

H_{Feynman} here represents Feynman's Hamiltonian introduced in Eq. 1. This Hamiltonian has the required groundstate $|\psi_{\text{hist}}\rangle = \frac{1}{\sqrt{k+1}} \sum_{t=0}^k |\psi_t\rangle$ which is a superposition of the $k+1$ orthonormal states $|\psi_t\rangle = |t\rangle_c \otimes U_t, \dots, U_1 |\psi_{in}\rangle$. The effective evolution of the clock is given by the clock Hamiltonian,

$$H_{\text{clock}(s)l,l'} = \begin{cases} s/2 & \text{if } l = l' = 0, \\ 1 & \text{if } l = l' \in \{1, \dots, k-1\}, \\ 1 - s/2 & \text{if } l = l' = k, \\ -s/2 & \text{if } |l - l'| = 1, \\ 0 & \text{otherwise.} \end{cases}$$

The gap in the spectrum between the ground state and the first excited state of this clock Hamiltonian determines how large T must be to ensure with high probability that the total system remains in the ground state, and the eventual evolution is given by H_{Feynman} . (In fact H_{Feynman} is defined slightly differently which is the reason that the evolution at $s = 1$ is not identical to our Hamiltonian 5). The minimum gap occurs at a time s which is slightly less than 1.

Appendix B: Feynman's Hamiltonian for $k = 2$

To understand the structure of the Hamiltonian and the time evolution operator, we look at the simplest example of having two operations on our register. For $k=2$, we add to the n atoms in our register a new set of 3 atoms, which we call 'program counter sites'. q_i and q_i^\dagger represent the annihilation and creation operators, respectively, for the program sites $i = 0, 1, 2$. Our Hamiltonian in matrix form is given by,

$$\hat{H}_{\text{TOT}} = \begin{pmatrix} 0 & 0 & 0 & 0 & 0 & 0 & 0 & 0 & 0 \\ 0 & 0 & \hat{U}_2 & 0 & 0 & 0 & 0 & 0 & 0 \\ 0 & \hat{U}_2^\dagger & 0 & 0 & \hat{U}_1 & 0 & 0 & 0 & 0 \\ 0 & 0 & 0 & 0 & 0 & \hat{U}_1 & 0 & 0 & 0 \\ 0 & 0 & \hat{U}_1^\dagger & 0 & 0 & 0 & 0 & 0 & 0 \\ 0 & 0 & 0 & 0 & \hat{U}_1^\dagger & 0 & 0 & \hat{U}_2 & 0 \\ 0 & 0 & 0 & 0 & 0 & 0 & \hat{U}_2^\dagger & 0 & 0 \\ 0 & 0 & 0 & 0 & 0 & 0 & 0 & 0 & 0 \end{pmatrix}. \quad (\text{B1})$$

This Hamiltonian relates to 2 independent clock spaces. The first is a program counter where at all times only one site is occupied, i.e $|100\rangle, |010\rangle, |001\rangle$. The second is a program counter where at all times two sites are occupied, i.e $|011\rangle, |101\rangle, |110\rangle$. The construction of Feynman's Hamiltonian ensures that the number of program sites occupied is a conserved quantity. This allows us to block-diagonalize the Hamiltonian into non-interacting blocks and separate out the part where only one clock site is occupied.

We will suppose that, in the operation of this computer, only one site is occupied for all time. We call this Hamiltonian \hat{H} and can extract it from our total Hamiltonian,

$$\hat{H} = \begin{bmatrix} 0 & \hat{U}_1^\dagger & 0 \\ \hat{U}_1 & 0 & \hat{U}_2^\dagger \\ 0 & \hat{U}_2 & 0 \end{bmatrix}. \quad (\text{B2})$$

This Hamiltonian satisfies the relation,

$$\hat{H}^3 = 2\hat{H}. \quad (\text{B3})$$

Using a Taylor expansion, the time evolution operator reduces to,

$$e^{-i\hat{H}t} = \hat{I} - i\frac{\hat{H}}{\sqrt{2}} \sin \sqrt{2}t + \frac{\hat{H}^2}{2} (\cos \sqrt{2}t - 1). \quad (\text{B4})$$

In matrix form this is,

$$e^{-i\hat{H}t} = \begin{bmatrix} 1 + \frac{\cos \sqrt{2}t - 1}{2} & \frac{i}{\sqrt{2}} \sin \sqrt{2}t \hat{U}_1^\dagger & \frac{\cos \sqrt{2}t - 1}{2} \hat{U}_1^\dagger \hat{U}_2^\dagger \\ \frac{-i}{\sqrt{2}} \sin \sqrt{2}t \hat{U}_1 & \cos \sqrt{2}t & \frac{-i}{\sqrt{2}} \sin \sqrt{2}t \hat{U}_2^\dagger \\ \frac{\cos \sqrt{2}t - 1}{2} \hat{U}_2 \hat{U}_1 & \frac{i}{\sqrt{2}} \sin \sqrt{2}t \hat{U}_2 & 1 + \frac{\cos \sqrt{2}t - 1}{2} \end{bmatrix}. \quad (\text{B5})$$

This matrix is unitary. When the program counter reaches the final site $|001\rangle$ the data register has been multiplied by the operators $\hat{U}_2 \hat{U}_1$ as expected. This occurs at $t = \frac{\pi}{\sqrt{2}}$.

Appendix C: Proving the Structure of a Hamiltonian

To prove the structure given in (6), we expand the time-evolution matrix,

$$\hat{G}(t) = \sum_{m=0}^{\infty} \frac{(-it)^m}{m!} \hat{H}^m. \quad (\text{C1})$$

Hence it is sufficient to prove that all powers of the Hamiltonian also follow the structure of (6), which will be done via a proof of induction. The method of extracting \hat{H} , wherein only one site of the clock space is occupied, may be extracted from \hat{H}_{TOT} in a similar manner to (B2). The first power of the Hamiltonian is then, by construction,

$$\hat{H} = \begin{bmatrix} 0 & \hat{U}_1^\dagger & & & & \\ \hat{U}_1 & 0 & \hat{U}_2^\dagger & & & \\ & \hat{U}_2 & 0 & \hat{U}_3^\dagger & & \\ & & & \ddots & \ddots & \ddots \\ & & & & \hat{U}_{k-1} & 0 & \hat{U}_k^\dagger \\ & & & & & \hat{U}_k & 0 \end{bmatrix}, \quad (\text{C2})$$

which clearly has the structure in (6). To prove that \hat{H}^{m+1} has this same structure assuming that \hat{H}^m does, we approach the problem case by case. Explicitly, each element is given by,

$$\begin{aligned} (\hat{H}^{m+1})_{ij} &= (\hat{H} \hat{H}^m)_{ij}, \\ &= \sum_l \hat{H}_{il} \hat{H}_{lj}^m, \\ &= \hat{H}_{i,i-1} \hat{H}_{i-1,j}^m + \hat{H}_{i,i+1} \hat{H}_{i+1,j}^m. \end{aligned}$$

For $i = j$, where $b_{ij}^{(m)}$ is the coefficient associated to $\hat{H}_{ij}^{(m)}$, where,

$$m = 1, b_{ij}^{(1)} = \begin{cases} 1 & \text{if } |i - j| = 1; \\ 0 & \text{otherwise,} \end{cases} \quad (\text{C3})$$

such that,

$$\begin{aligned} (\hat{H}^{m+1})_{ii} &= b_{i-1,i}^{(m)} \hat{U}_{i-1} \hat{U}_{i-1}^\dagger + b_{i+1,i}^{(m)} \hat{U}_i \hat{U}_i^\dagger, \\ &= (b_{i-1,i}^{(m)} + b_{i+1,i}^{(m)}) \mathbb{I}, \end{aligned}$$

where we have used the identity $U_i^\dagger U_i = \mathbb{I}$ to reduce the string length. Similarly, for $0 \leq i < j \leq k$,

$$\begin{aligned} (\hat{H}^{m+1})_{ij} &= b_{i-1,j}^{(m)} \hat{U}_{i-1} \hat{U}_{i-1}^\dagger \hat{U}_i^\dagger \dots \hat{U}_{j-1}^\dagger + b_{i+1,j}^{(m)} \hat{U}_i \hat{U}_i^\dagger \dots \hat{U}_{j-1}^\dagger \\ &= (b_{i-1,j}^{(m)} + b_{i+1,j}^{(m)}) \hat{U}_i \hat{U}_i^\dagger \dots \hat{U}_{j-1}^\dagger. \end{aligned}$$

Likewise, for $0 \leq j < i \leq k$,

$$\begin{aligned} (\hat{H}^{m+1})_{ij} &= b_{i-1,j}^{(m)} \hat{U}_{i-1} \dots \hat{U}_j + b_{i+1,j}^{(m)} \hat{U}_i \hat{U}_i^\dagger \hat{U}_{i-1} \dots \hat{U}_j \\ &= (b_{i-1,j}^{(m)} + b_{i+1,j}^{(m)}) \hat{U}_{i-1} \dots \hat{U}_j. \end{aligned}$$

Hence each power of the Hamiltonian has the same structure as (6), and therefore $\hat{G}(t)$ must also have the same structure. Note that this derivation also proves that the clock Hamiltonian is given by (7).

Appendix D: Analytic solution of $P_k(\tau)$

Using $\hat{G}(t) = e^{-i\hat{H}t}$ and the eigenvalues and eigenvectors given in (9), an analytic solution for $P_k(t)$ can be found,

$$\begin{aligned} P_k(t) &= |\langle k | \hat{G}(t) | 0 \rangle|^2 \\ &= \left| \sum_n \sum_j \langle k | \psi_n \rangle \langle \psi_n | e^{-i\hat{H}_{eff}t} | \psi_j \rangle \langle \psi_j | 0 \rangle \right|^2 \\ &= \left| \sum_n \sum_j \langle k | \psi_n \rangle \langle \psi_n | e^{-i\lambda_j t} | \psi_j \rangle \langle \psi_j | 0 \rangle \right|^2 \\ &= \left| \sum_j e^{-i\lambda_j t} \langle k | \psi_j \rangle \langle \psi_j | 0 \rangle \right|^2 \\ &= \left| \frac{2}{k+1} \sum_{j=0}^k e^{-i\lambda_j t} \sin^2 \frac{\pi(j+1)}{k+1} (-1)^j \right|^2. \end{aligned} \quad (\text{D1})$$

In the following, we assume that k is an even number. The derivation for odd k is analogous. Starting from the expression for $a_{k0}(t)$ given in (10), we split the sum into two parts,

$$\begin{aligned} a_{k0} &= \frac{2}{k+1} \sum_{j=0}^{\frac{k}{2}} e^{-i\lambda_j t} \sin^2 \frac{\pi(j+1)}{k+1} (-1)^j \\ &\quad + \frac{2}{k+1} \sum_{j=\frac{k}{2}+1}^k e^{-i\lambda_j t} \sin^2 \frac{\pi(j+1)}{k+2} (-1)^j. \end{aligned} \quad (\text{D2})$$

By a change of variable $j = k+1 - m$ in the second term,

$$\begin{aligned} a_{k0} &= \frac{2}{k+1} \sum_{m=0}^{\frac{k}{2}} e^{-i\lambda_m t} \sin^2 \frac{\pi(m+1)}{k+1} (-1)^m \\ &\quad - \frac{2}{k+1} \sum_{m=0}^{\frac{k}{2}} e^{+i\lambda_m t} \sin^2 \frac{\pi(m+1)}{k+1} (-1)^{k+1-m} \\ &= \frac{2}{k+1} \sum_{m=0}^{\frac{k}{2}} (e^{-i\lambda_m t} - e^{+i\lambda_m t}) \sin^2 \frac{\pi(m+1)}{k+1} (-1)^m \\ &= \frac{-4i}{k+1} \sum_{m=0}^{\frac{k}{2}} \sin \lambda_m t \sin^2 \frac{\pi(m+1)}{k+1} (-1)^m \end{aligned} \quad (\text{D3})$$

Substituting in (9) the (approximate) optimal time $\tau = \frac{k+1}{2}$, we get

$$\begin{aligned} a_{k0} &= \frac{-4i}{k+1} \sum_{m=0}^{\frac{k}{2}} \sin \left((k+1) \cos \left(\frac{\pi(m+1)}{k+1} \right) \right) \\ &\quad \times \sin^2 \frac{\pi(m+1)}{k+1} (-1)^m \end{aligned}$$

Using another change of variable, we set $p = \frac{k}{2} - m$,

$$\begin{aligned} a_{k0} &= \frac{-4i}{k+1} \sum_{p=0}^{\frac{k}{2}} \sin \left((k+1) \sin \left(\frac{\pi(2p-1)}{2(k+1)} \right) \right) \\ &\quad \times \cos^2 \left(\frac{\pi(2p-1)}{2(k+1)} \right) (-1)^{\frac{k}{2}-p} \end{aligned}$$

To estimate this sum, we do a second-order Taylor expansion of the argument of the outer sine-function:

$$(k+1) \sin\left(\frac{\pi(2p-1)}{2(k+1)}\right) \approx \left(p - \frac{1}{2}\right)\pi - \frac{\pi^3}{6(k+1)^2} \left(p - \frac{1}{2}\right)^3 \quad (\text{D4})$$

Then noting that $\sin\left(\pi\left(p - \frac{1}{2}\right) - a\right) = (-1)^{p-1} \cos(a)$, we obtain

$$a_{(k+1)1} = \frac{4i(-1)^{\frac{k}{2}}}{k+1} \sum_{p=1}^{\frac{k}{2}} \cos^2\left(\frac{\pi(2p-1)}{2(k+1)}\right) (-1)^{\frac{k}{2}-p} \times \cos\left(\frac{\pi^3}{6(k+1)^2} \left(p - \frac{1}{2}\right)^3\right). \quad (\text{D5})$$

This is formula (11). We now note that the second cosine factor is rapidly oscillating for large k . This means that large p -values make a negligible contribution. For small values, the first cosine factor is almost equal to 1 and can be omitted. Introducing the variable $x = \frac{\pi}{(k+2)^{2/3}} \left(p - \frac{1}{2}\right)$, we can approximate the sum by a Riemann integral:

$$a_{k0} \approx \frac{4i(-1)^{\frac{k}{2}}}{\pi(k+1)^{1/3}} \int_0^\infty \cos\left(\frac{1}{6}x^3\right) dx. \quad (\text{D6})$$

The integral can be evaluated using integration by parts, and we obtain

$$a_{k0} \approx 2.27i(-1)^{k/2} k^{-1/3}. \quad (\text{D7})$$

Squaring this yields (12). There is a difference between our theoretical coefficient of 5.14 and the numerical value of 6.76. This is due to the approximate form in (D5). Our approximation here holds best at large k and coefficients are expected to show better agreement in this regime.

Appendix E: Predicting the Location of the Second Maximum

In Appendix D, we found that the first maximum occurs approximately at $\tau = \frac{1}{2}(k+1)$. At this value for t ,

$$2t \left(\frac{(2p-1)\pi}{2(k+1)} - \frac{1}{6} \left(\frac{\pi(2p-1)}{2(k+1)} \right)^3 \right) \approx \left(p - \frac{1}{2} \right) \pi \quad (\text{E1})$$

which is an odd multiple of $\pi/2$. The next maximum should occur when

$$2t \left(\frac{(2p-1)\pi}{2(k+1)} - \frac{1}{6} \left(\frac{\pi(2p-1)}{2(k+1)} \right)^3 \right) \approx \left(p + \frac{1}{2} \right) \pi. \quad (\text{E2})$$

Setting $t = (k+2)(1+\delta)/2$, this becomes

$$\delta \frac{2p-1}{2} - \frac{\pi^2(2p-1)^3}{48(k+1)^2} \approx 1 \quad (\text{E3})$$

On the other hand, we want this to remain a good approximation if we increase or decrease p . This is the case if we set

$$2t \frac{d}{dp} \left(\frac{(2p-1)}{2(k+1)} - \frac{\pi^2}{6} \left(\frac{p-\frac{1}{2}}{k+1} \right)^3 \right) = 1 \quad (\text{E4})$$

i.e increasing p by 1 also increases the left-hand side by 1. Hence,

$$2t \left(\frac{1}{k+1} - \frac{\pi^2}{2} \frac{\left(p - \frac{1}{2}\right)^2}{(k+1)^3} \right) = 1. \quad (\text{E5})$$

Inserting $2t = (k+1)(1+\delta)$ we get

$$\delta \approx \frac{\pi^2}{2} \frac{\left(p - \frac{1}{2}\right)^2}{(k+1)^2}. \quad (\text{E6})$$

Combining this with the previous identity we obtain

$$\frac{\pi^2}{24} \frac{(2p-1)^3}{(k+1)^2} = 1. \quad (\text{E7})$$

Finally inserting this into δ , we get

$$\delta = 0.5(3\pi)^{2/3} (k+1)^{-2/3} = 2.23(k+1)^{-2/3}. \quad (\text{E8})$$